

Heterotrinnuclear Complexes of the Platinum Group Metals with 2,2'-Biimidazole as a Bridging Ligand

Andrey Mayboroda,^[a] Peter Comba,^{*[a]} Hans Pritzkow,^[a] Gerd Rheinwald,^[b] Heinrich Lang,^[b] and Gerard van Koten^[c]

Keywords: Osmium / Platinum / Palladium / Heterometallic complexes / Cyclic voltammetry / Hydrogenation

The novel trinuclear complexes [(Pt{C₆H₃(CH₂NMe₂-2,6)₂})₂(μ-Hbiim)₂Os(O=PPh₃)₂](NO₃)(SO₃CF₃)₂ [C₆H₃(CH₂NMe₂-2,6)₂ = pincer ligand, H₂biim = 2,2'-biimidazole] and [(PdL)₂(μ-biim)₂Os(O=PPh₃)₂](NO₃)₃ (L = cod, 1,5-cyclooctadiene or L = en, ethylene-1,2-diamine) were prepared by the reaction of the mononuclear complex [Os(H₂biim)₂(O=PPh₃)₂](NO₃)₃ with [Pt{C₆H₃(CH₂NMe₂-2,6)₂}(SO₃CF₃)], or with PdL(NO₃)₂ (L = cod or L = en), in the presence of a base. The exchange reaction between [Os(Hbiim)₂(O=PPh₃)₂](NO₃)₃ and [Me₂NH₂][RhCl₄(NHMe₂)] led to the formation of [Os(Hbiim)₂(O=PPh₃)₂][RhCl₄(NHMe₂)]. The solid-state structures of [Os(Hbiim)₂(O=PPh₃)₂][RhCl₄(NHMe₂)] and [(Pt{C₆H₃(CH₂NMe₂-2,6)₂})₂(μ-Hbiim)₂Os(O=PPh₃)₂](NO₃)(SO₃CF₃)₂·4H₂O were determined by single-crystal X-ray diffraction. The crystals of [Os(Hbiim)₂(O=PPh₃)₂][RhCl₄(NHMe₂)] are triclinic with a space group *P* $\bar{1}$,

with *a* = 10.4293(5), *b* = 10.6365(6), *c* = 13.0287(7) Å, β = 91.6840(10), γ = 109.8540(10)°, *V* = 1316.14(12) Å³, *Z* = 1. The crystals of the complex [(Pt{C₆H₃(CH₂NMe₂-2,6)₂})₂(μ-Hbiim)₂Os(O=PPh₃)₂](NO₃)(SO₃CF₃)₂·4H₂O are triclinic with a space group *P* $\bar{1}$, with *a* = 12.604(3), *b* = 13.471(3), *c* = 14.347(3) Å, β = 77.530(5), γ = 66.613(4)°, *V* = 2005.6(7) Å³, *Z* = 1. Deprotonation of 2,2'-biimidazole in the mononuclear osmium complex, followed by coordination to an additional transition metal fragment leads to a modification of the ligand field and a variation of the redox properties of the Os^{III} center. [(Pd(cod))₂(μ-biim)₂Os(O=PPh₃)₂](NO₃)₃ shows significant catalytic activity towards hydrogenation of terminal and cyclic alkenes.

(© Wiley-VCH Verlag GmbH & Co. KGaA, 69451 Weinheim, Germany, 2003)

Introduction

Oligonuclear complexes in which the transition-metal centers are bridged by π-conjugated ligands have attracted much attention as model compounds for the study of cooperative effects in, for example, homogeneous catalysis.^[1] Mechanisms have been postulated which involve more than one catalytically active metal center within the oligometallic array.^[2] Generally, however, only one of the metal centers plays a dominant role in the catalytic cycle, while the other(s) influence the molecular architecture and support the catalytically active center as a donor or acceptor of electron density. An enhancement of the reactivity results from changes in the ligand field or from intramolecular electronic communication between the transition-metal centers.^[1b]

Much attention has been focused on the metal-binding ability of the ligand 2,2'-biimidazole (H₂biim) and its derivatives.^[3–9] Anionic moieties, e.g. Hbiim[−] and biim^{2−}, have successfully been used as bridging ligands for the synthesis of homo- and heterometallic oligonuclear complexes. Dinuclear 2,2'-biimidazolate complexes of Rh^I,^[3] Ir^I,^[3] Cu^{II},^[4] Pd^{II},^[5,6] Ru^{II},^[7] Ru^{II}-Os^{II},^[8] and Ru^{II}-Rh^I^[9] have been prepared and characterized. An example of a trinuclear heterometallic species of the structural type **A** is [(Au(PPh₃)₂)(μ-bbzim)Rh(cod)](ClO₄) (bbzim = 2,2'-bi-benzimidazole).^[9] However, so far there are no examples of trinuclear complexes of types **B** and **C** (Figure 1).

Here, we report on the synthesis and characterization of the Pt^{II}-Os^{III}-Pt^{II} and Pd^{II}-Os^{III}-Pd^{II} complexes, with 2,2'-biimidazolate (Hbiim[−], biim^{2−}) as the bridging ligands (structural types **B** and **C**). The solid-state structures of [Os(Hbiim)₂(O=PPh₃)₂][RhCl₄{NH(CH₃)₂}₂] (**2b**) and [(Pt{C₆H₃(CH₂NMe₂-2,6)₂})₂(μ-Hbiim)₂Os(O=PPh₃)₂](NO₃)(SO₃CF₃)₂·4H₂O (**7**) are reported (for the numbering of the complexes, see Scheme 1, cod = 1,5-cyclooctadiene, en = ethylene-1,2-diamine). The electrochemical behavior of compounds **7–9** was studied, using cyclic voltammetry, and the catalytic activity of **7–9**, in the homogeneous hydrogenation of 1-hexene and cyclohexene, is also reported.

^[a] Anorganisch-Chemisches Institut, Universität Heidelberg, Im Neuenheimer Feld 270, 69120 Heidelberg, Germany
E-mail: comba@akcomba.oci.uni-heidelberg.de

^[b] Technische Universität Chemnitz, Fakultät für Naturwissenschaften, Institut für Chemie, Lehrstuhl Anorganische Chemie, Straße der Nationen 62, 09111 Chemnitz, Germany

^[c] Debye Institute, Department of Metal-Mediated Synthesis, Utrecht University, Padualaan 8, 3584 CH Utrecht, The Netherlands

Supporting information for this article is available on the WWW under <http://www.eurjic.org> or from the author.

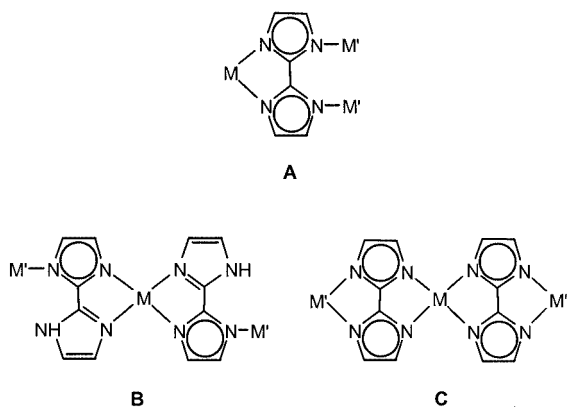


Figure 1. Type A–C trinuclear complexes with different binding modes between 2,2'-biimidazole and the transition metal centers M and M'

Results and Discussion

Synthesis and Spectroscopy

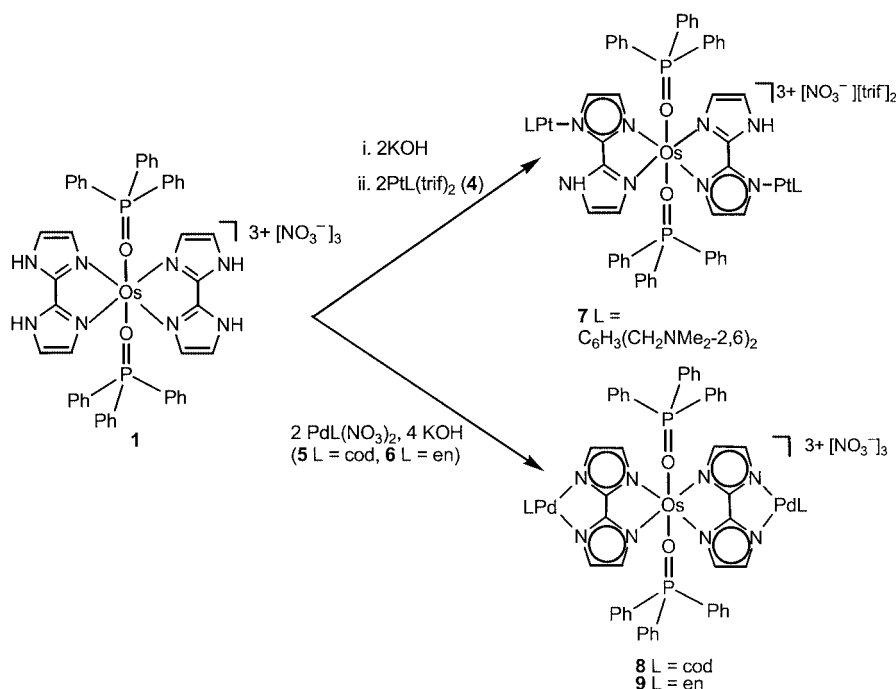
The mononuclear osmium(III) complex $[\text{Os}(\text{H}_2\text{biim})_2(\text{O}=\text{PPh}_3)_2](\text{NO}_3)_3$ (**1**),^[10] was used as a starting material in the synthesis of the trimetallic OsPt₂ and OsPd₂ complexes **7–9**. Complex **1** is a polybasic acid and was successfully deprotonated by KOH, affording $[\text{Os}(\text{Hbiim})_2(\text{O}=\text{PPh}_3)_2](\text{NO}_3)_3$ (**2**),^[10] and $[\text{Os}(\text{biim})_2(\text{O}=\text{PPh}_3)_2]^-$ (**3**, not isolated as a solid). Complexes **2** and **3** are reactive building blocks (“metal complex as the ligand”), which smoothly reacted with various transition-metal complexes, producing the trimetallic compounds **7–9** in high yields (Scheme 1). After appropriate workup, complexes **7–9** were isolated as

red (**7**) or dark green (**8, 9**) air-stable solids, which gradually decompose at temperatures higher than 150 °C. They are insoluble in tetrahydrofuran, acetone, diethyl ether and aromatic hydrocarbons, only moderately soluble in methanol and dichloromethane, but very soluble in a mixture of these solvents, e.g., in 80% of dichloromethane and 20% of methanol.

We were also interested in the structural properties of mononuclear osmium(III) complexes with a partially deprotonated 2,2'-biimidazole ligand. Attempts to crystallize $[\text{Os}(\text{Hbiim})_2(\text{O}=\text{PPh}_3)_2](\text{NO}_3)_3$ (**2a**) from dichloromethane/methanol were unsuccessful. However, in the presence of the rhodium(III) salt $[\text{Me}_2\text{NH}_2][\text{RhCl}_4\{\text{NH}(\text{CH}_3)_2\}_2]$ (**10**) single crystals of $[\text{Os}(\text{Hbiim})_2(\text{O}=\text{PPh}_3)_2][\text{RhCl}_4(\text{NH}(\text{CH}_3)_2)_2]$ (**2b**), suitable for X-ray structure determination, could be obtained (see below).

The UV/Vis spectra of **7–9** have an absorbance maximum at approx. 350 nm, which can be assigned to a metal-to-ligand charge-transfer transition {for comparison, the parent complex $[\text{Os}(\text{H}_2\text{biim})_2(\text{O}=\text{PPh}_3)_2](\text{NO}_3)_3$ (**1**) has two transitions at 360 and 388 nm^[10]. In the visible region, a broad absorbance of low intensity at approx. 550 nm is also observed for **8** and **9**, and these are assigned to d-d transitions. It is worth noting that the mononuclear Os^{III} complex **1**, as well as the Pt^{II} and Pd^{II} complexes **4–6**, have no transitions in this region.

The infrared spectrum of 2,2'-biimidazole shows a strong absorption band at around 3100 cm⁻¹, which is assigned to the N–H stretching vibrations. This band is also found in the infrared spectrum of **7** (at 3075 cm⁻¹), however, it is not observed in the infrared spectra of **8** and **9**. This implies that complete deprotonation of the 2,2'-biimidazole bridging ligands occurs in the trinuclear compounds **8** and **9**.



Scheme 1

The effective magnetic moments of the trinuclear complexes [$\mu_{\text{eff}} = 1.87$ (**7**), 1.45 (**8**), 1.58 (**9**) BM; powders, 298 K] are as expected for Os^{III} complexes (one unpaired electron, 1.73 BM). Complex **7** could not be characterized by NMR spectroscopy, owing to its magnetic properties. The paramagnetism of complexes **8** and **9** leads to considerable broadening of the NMR signals, but these spectra are sufficiently resolved to be interpreted. The ^1H NMR spectra of $[\{\text{Pd}(\text{cod})\}_2(\mu\text{-biim})_2\text{Os}(\text{O}=\text{PPh}_3)_2](\text{NO}_3)_3$ (**8**) and $[\{\text{Pd}(\text{en})\}_2(\mu\text{-biim})_2\text{Os}(\text{O}=\text{PPh}_3)_2](\text{NO}_3)_3$ (**9**) show a multiplet between $\delta = 7.5$ and 7.8 ppm, due to the superimposition of the signals resulting from the Ph_3PO and biim fragments. The resonance signals at $\delta = 2.5$ and 5.5 ppm, also observed in the ^1H NMR spectrum of **8**, can be assigned to the CH and CH_2 groups, respectively, of the coordinated cyclooctadiene. They are slightly shifted to a lower field compared to those in the spectrum of the metal-free ligand. In the spectrum of complex **9**, the resonance signal for the CH_2 groups of the en ligands is observed at $\delta = 2.96$ ppm, while in the spectrum of metal-free en, the signal of these protons appears at $\delta = 2.85$ ppm. The carbon resonance signals of the terminal cod ($\delta = 28.4$, 76.4 ppm) and en units ($\delta = 47.3$ ppm), observed in the $^{13}\text{C}\{^1\text{H}\}$ NMR spectra of **8** and **9**, respectively, are also shifted to a lower field, when compared with the spectra of the corresponding metal-free ligands. As a result of the deprotonation of H_2biim and the addition of the PdL complex fragments, the ^{13}C resonances of 2,2'-biimidazole are shifted to a lower field in comparison with **1**. The signal for the C atoms in the 2, 2'-position is observed at $\delta = 152.1$ ppm (**8**) and at $\delta = 152.6$ ppm (**9**), while this resonance is found at $\delta = 141.2$ ppm for **1**. The variation of the terminal ligand coordinated to the palladium center does not affect the chemical shifts of the C atoms in the 2,2'-biimidazolate bridging ligands.

In the $^{31}\text{P}\{^1\text{H}\}$ NMR spectra of **8** and **9**, the signal for the phosphorus atom of the triphenylphosphane oxide group is seen at $\delta = 32.6$ ppm. Relative to $[\text{Os}(\text{H}_2\text{biim})_2(\text{O}=\text{PPh}_3)_2](\text{NO}_3)_3$ (**1**) this ^{31}P signal is shifted to a higher field by approx. 3.8 ppm and this indicates an increase of electron density at the Os^{III} center due to better electron donation of the deprotonated 2,2'-biimidazole ligand.

Electrochemistry

Cyclic voltammetric studies of **1** and **7–9** were carried out in methanol at 25 °C. The mononuclear complex $[\text{Os}(\text{H}_2\text{biim})_2(\text{O}=\text{PPh}_3)_2](\text{NO}_3)_3$ (**1**) has a reversible one-electron step at $E_{1/2} = -1.01$ V (vs. Fc/Fc^+ , Figure 2, a). This is attributed to the $\text{Os}^{\text{II}}/\text{Os}^{\text{III}}$ redox couple. Complex **1** also has an irreversible $\text{Os}^{\text{III}}/\text{Os}^{\text{IV}}$ oxidation at 0.92 V. In contrast to this, the trinuclear complexes **7–9** have a single quasi-reversible voltammetric response (Figure 2, b shows the cyclic voltammogram of **8** as an example). Since $[\text{Pt}\{\text{C}_6\text{H}_3(\text{CH}_2\text{NMe}_2-2,6)_2\}_2(\text{SO}_3\text{CF}_3)(\text{O}=\text{PPh}_3)_2](\text{NO}_3)(\text{SO}_3\text{SF}_3)_2 \cdot 4\text{H}_2\text{O}$ (**4**), $[\text{Pd}(\text{cod})(\text{H}_2\text{biim})](\text{NO}_3)_2$ (**5**) and $[\text{Pd}(\text{en})(\text{H}_2\text{biim})](\text{NO}_3)_2$ (**6**) do not have a cyclic voltammetric response in the potential range -1.2 to $+1.2$ V, the processes observed in the

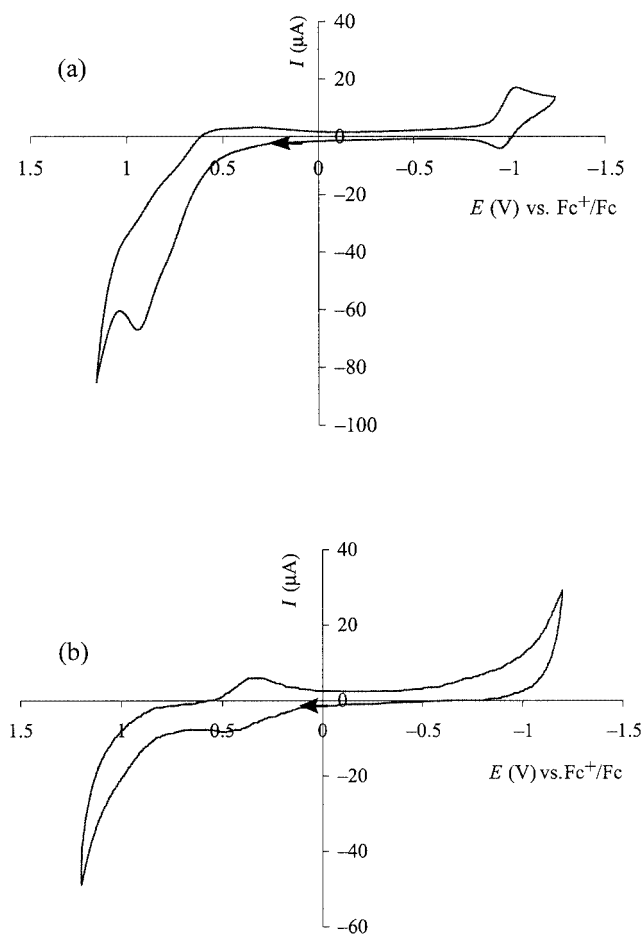


Figure 2. Cyclic voltammograms of (a) $[\text{Os}(\text{H}_2\text{biim})_2(\text{O}=\text{PPh}_3)_2](\text{NO}_3)_3$ (**1**) and (b) $[\{\text{Pd}(\text{cod})\}_2\text{Os}(\mu\text{-biim})_2(\text{O}=\text{PPh}_3)_2](\text{NO}_3)_3$ (**8**)

cyclic voltammograms of **7–9** are attributed to the $\text{Os}^{\text{III}}/\text{Os}^{\text{IV}}$ redox couple. Electrochemical data are given in Table 1.

Table 1. Electrochemical data of **1** and **7–9**

Complex ^[a]	$E_{1/2}(\text{Os}^{\text{III}}/\text{Os}^{\text{IV}})$ [V]
$[\text{Os}(\text{H}_2\text{biim})_2(\text{O}=\text{PPh}_3)_2](\text{NO}_3)_3$ (1)	0.92
$[\{\text{Pt}\{\text{C}_6\text{H}_3(\text{CH}_2\text{NMe}_2-2,6)_2\}_2\text{Os}(\mu\text{-Hbiim})_2(\text{O}=\text{PPh}_3)_2](\text{NO}_3)(\text{SO}_3\text{SF}_3)_2 \cdot 4\text{H}_2\text{O}$ (7)	0.53
$[\{\text{Pd}(\text{cod})\}_2\text{Os}(\mu\text{-biim})_2(\text{O}=\text{PPh}_3)_2](\text{NO}_3)_3$ (8)	0.41
$[\{\text{Pd}(\text{en})\}_2\text{Os}(\mu\text{-biim})_2(\text{O}=\text{PPh}_3)_2](\text{NO}_3)_3$ (9)	0.23

[a] CH_3OH , 25 °C, vs. $E(\text{Fc}/\text{Fc}^+) = 0.00$ V.

The addition of transition-metal fragments such as $[\text{Pd}(\text{cod})]^{2+}$ or $[\text{Pd}(\text{en})]^{2+}$ to **3** leads to a significant cathodic shift of the $\text{Os}^{\text{III}}/\text{Os}^{\text{IV}}$ couple (Table 1). For **9**, this occurs at a more negative potential ($E_{1/2} = +0.23$ V) than that for **8** ($E_{1/2} = +0.41$ V). However, NMR spectroscopy shows that substitution of cod by en in PdL does not affect the chemical shifts of the C atoms in the biimidazolate bridging

group, and the chemical shifts of the P atoms in $\text{Ph}_3\text{P}=\text{O}$ in **8** and **9** are also almost identical. Therefore, it is not appropriate to attribute the difference in the redox potentials of **8** and **9** to an effect of the terminal ligand (cod, en) on the osmium center. Possible reasons for the shift in the redox potential are a variation of the adsorption properties of the complex cation at the electrode or of the electron transfer between the electrode and the osmium complex as a function of the terminal ligands.

Solid-State Structures

Slow concentration of dichloromethane/methanol solutions of $[\text{Os}(\text{Hbiim})_2(\text{O}=\text{PPh}_3)_2][\text{RhCl}_4\{\text{NH}(\text{CH}_3)_2\}_2]$ (**2b**) and $[(\text{Pt}\{\text{C}_6\text{H}_3(\text{CH}_2\text{NMe}_2-2,6)_2\})_2(\mu\text{-Hbiim})_2\text{Os}(\text{O}=\text{PPh}_3)_2](\text{NO}_3)(\text{SO}_3\text{CF}_3)_2\cdot 4\text{H}_2\text{O}$ (**7**) led to the formation of red crystals of **2b** and pale pink crystals of **7**, respectively. Both **2b** and **7** crystallize in triclinic space groups $P\bar{1}$. The coordination geometry around the osmium center in the two complexes is approximately octahedral. The polyhedron is defined by the four nitrogen atoms of two Hbiim⁻ ligands and the two oxygen atoms of the $\text{Ph}_3\text{P}=\text{O}$ units, which are in the axial positions.

Figure 3 shows the ZORTEP^[11] plot of complex **2b**; structural parameters are given in Table 2. The $[\text{Os}(\text{Hbiim})_2(\text{O}=\text{PPh}_3)_2]^+$ cation and the $[\text{RhCl}_4\{\text{NH}(\text{CH}_3)_2\}_2]^-$ anion have a center of inversion, located at the osmium and rhodium centers, respectively; the symmetry-generated atoms are identified with the suffix a. The Os(1)–N(1) and Os(1)–N(3) distances in **2b** (bonds to the mono-deprotonated 2,2'-biimidazolite ligands), are nearly identical to those in $[\text{Os}(\text{H}_2\text{biim})_2(\text{O}=\text{Ph}_3)_2](\text{NO}_3)_3$ (**1**) [**2**: Os(1)–N(1) = 2.076(2), Os(1)–N(3) = 2.080(2); **1**: Os(1)–N(1) = 2.0651(19) Å^[10]]. The deprotonated imidazolite sites in **2b** are *trans*-oriented. The Os(1)–O(1) bond [2.056(2) Å] is significantly longer than that observed in **1** and in other osmium complexes with a triphenylphosphane oxide, e.g., $[\text{Os}(\text{OEP})(\text{O}=\text{PPh}_3)_2]$ (Os–O = 2.036 Å, OEP = octaethylporphyrin).^[12] The bite angle N(1)–Os(1)–N(3) [77.78(6)°] is almost identical to that found in **1** [77.14(8)°] and is typical for bite angles in biimidazole and biimidazolato transition-metal complexes, e.g., $[\text{H}(\text{CO})(\text{PPh}_3)_2\text{Ru}(\mu\text{-biim})\text{Rh}(\text{cod})]$ [N–Ru–N = 79.2(2) Å]^[9] and $[\text{OsCl}(\eta^2\text{-H}_2)(\text{H}_2\text{biim})_2(\text{PtC}_3\text{H}_7)_2]\text{Cl}$ [N–Os–N = 75.6(3)°].^[13] The Rh^{III} ion in the counterion $[\text{RhCl}_4(\text{NHMe}_2)_2]^-$ in **2b** has a slightly distorted octahedral coordination geometry, where the chloride ions are situated in the equatorial positions and the amine groups are occupying the axial positions. The Rh(1)–Cl(1) [2.3597(5) Å] and Rh(1)–N(5) [2.106(2) Å] distances are in agreement with the bond lengths observed in similar octahedral Rh^{III} complexes, e.g., $[\text{ImH}][\text{RhCl}_4(\text{Im})_2]$ (Im = imidazole), with Rh–Cl = 2.326(2) Å and Rh–N = 2.039(4) Å.^[14] In the $[\text{RhCl}_4(\text{NHMe}_2)_2]^-$ anion, the four chloride ligands form an almost ideal quadrangle around the Rh atom [$\text{Cl}(1)\text{–Rh}(1)\text{–Cl}(2) = 92.979(2)^\circ$].

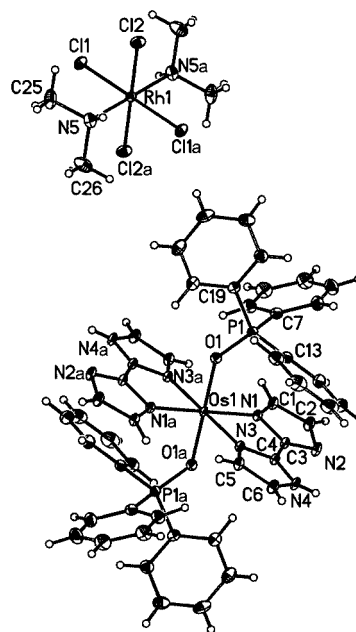


Figure 3. ZORTEP^[11] diagram of $[\text{Os}(\text{Hbiim})_2(\text{O}=\text{PPh}_3)_2][\text{RhCl}_4\{\text{NH}(\text{CH}_3)_2\}_2]$ (**2b**) (50% probability level); symmetry transformations used to generate equivalent atoms: $a = -x + 1, -y + 1, -z + 1$; $b = -x + 2, -y, -z + 2$

Table 2. Selected geometric parameters of $[\text{Os}(\text{Hbiim})_2(\text{O}=\text{PPh}_3)_2][\text{RhCl}_4\{\text{NH}(\text{CH}_3)_2\}_2]$ (**2b**) and $[(\text{Pt}\{\text{NMe}_2\}_2\text{CH}_2\}_2\text{C}_6\text{H}_3)_2(\mu\text{-Hbiim})_2\text{Os}(\text{O}=\text{PPh}_3)_2](\text{NO}_3)(\text{OTf})_2\cdot 4\text{H}_2\text{O}$ (**7**)

	2b	7
Distances [Å]		
Os1–O1	2.056(2)	2.030(5)
Os1–N1	2.076(2)	2.060(5)
Os1–N3	2.080(2)	2.076(5)
P1–O1	1.520(2)	1.513(5)
N1–C1	1.373(3)	1.341(9)
N1–C3	1.367(2)	1.362(6)
N2–C2	1.386(3)	1.380(9)
N2–C3	1.334(2)	1.331(8)
N3–C4	1.350(2)	1.341(8)
N3–C5	1.386(2)	1.386(8)
N4–C4	1.341(2)	1.335(8)
N4–C6	1.382(3)	1.366(9)
C1–C2	1.380(3)	1.376(10)
C5–C6	1.368(3)	1.350(9)
Pt1–N2		2.130(6)
Pt1–N5		2.090(6)
Pt1–N6		2.080(6)
Pt1–C25		1.949(6)
Angles [°]		
O1–Os1–N1	97.61(6)	92.0(2)
O1–Os1–N3	94.38(6)	95.32(19)
N1–Os1–N3	77.78(6)	78.3(2)
P1–O1–Os1	138.34(9)	147.4(3)
N2–Pt1–C25		175.2(3)
N5–Pt1–N6		163.1(2)

The crystal structure of **7** consists of the trimetallic OsPt_2 cation $[(\text{Pt}\{\text{NMe}_2\}_2\text{CH}_2\}_2\text{C}_6\text{H}_3)_2(\mu\text{-Hbiim})_2\text{Os}(\text{O}=\text{PPh}_3)_2]^{3+}$ with a nitrate and two triflate counterions and

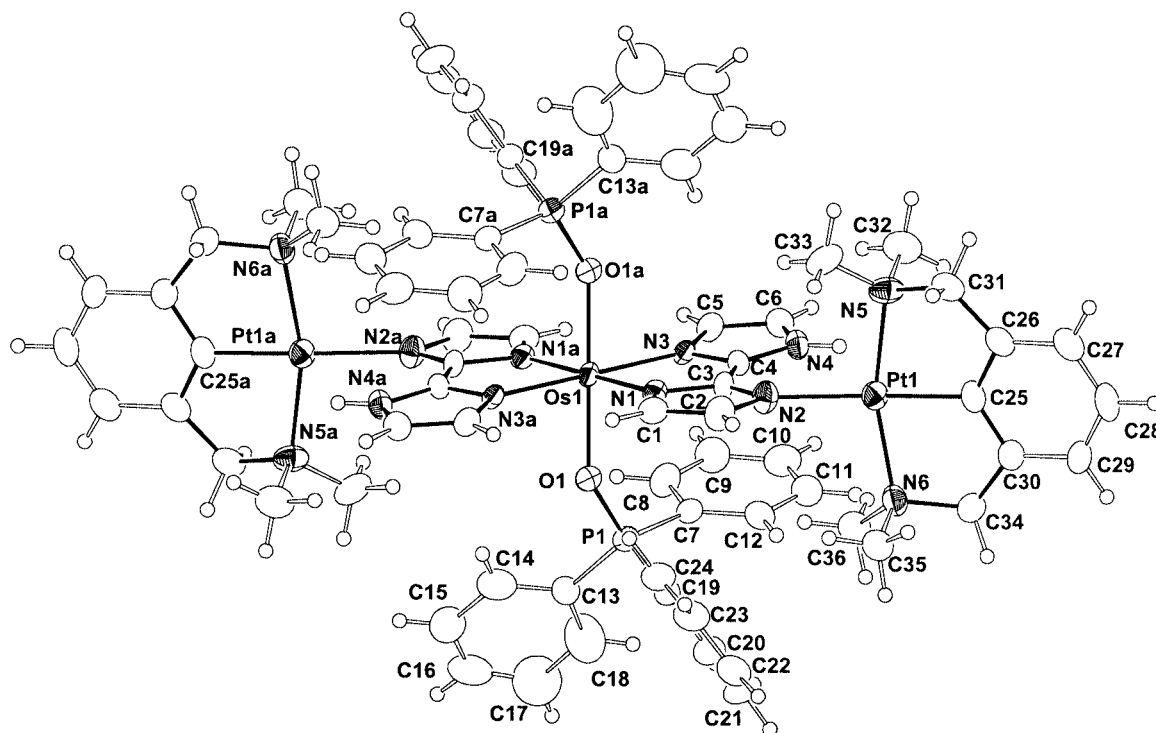


Figure 4. ZORTEP^[11] drawing of the complex cation $[(\text{Pt}\{\text{C}_6\text{H}_3(\text{CH}_2\text{NMe}_2\text{-}2,6)_2\})_2\text{Os}(\mu\text{-Hbiim})_2(\text{O}=\text{PPh}_3)_2]^{3+}$ of **7** (50% probability level; NO_3^- , SO_3CF_3^- and H_2O are omitted for clarity); symmetry transformation used to generate equivalent atoms: $a = -x + 1, -y + 1, -z$; $b = -x + 2, -y, -z$

four water molecules in the unit cell. A plot of the molecular cation with the atom numbering scheme is given in Figure 4, selected bond lengths and angles are listed in Table 2. The molecular cation **7** has a center of inversion situated at the osmium atom; symmetry-generated atoms are identified with the suffix *a*.

Each Hbiim⁻ bridging ligand in **7** is planar [root mean squares deviation rms = 0.0547 Å]. The Os(1)–N(1) and Os(1)–N(2) distances are slightly shorter than in **2b**, the bite angles of the Os–biim fragment are, as expected, nearly identical to those in **2b**. However, some changes are observed in the geometry of the triphenylphosphane oxide ligands. The Os(1)–O(1) distance in **7** is shorter than that in **2b** by 0.026 Å, and the P(1)–O(1)–Os(1) angle is larger than that in **2b** by 9.06°. The rigid biimidazole ligand is not affected. The PtL entities are planar [rms deviation = 0.0389 Å, Pt(1)–N(2)–N(5)–N(6)–C(25)] and are *trans*-

disposed, similar to the deprotonated sites in $[\text{Os}(\text{Hbiim})_2(\text{O}=\text{PPh}_3)_2]^+$ in **2b** (see Figure 3). The platinum centers have a slightly distorted square-planar coordination geometry. The N(5)–Pt(1)–N(6) angle is 163.1(4)°, which is in the typical range for NCN pincer complexes.^[15] The PtL units are perpendicular to the imidazole rings [interplanar angle between Pt(1)–N(2)–N(5)–N(6)–C(25) and N(1)–N(2)–C(1)–C(2)–C(3) = 89.14(25)°].

Catalytic Activity

The catalytic properties of the trimetallic complexes **7–9** were investigated through the homogeneous hydrogenation of 1-hexene and cyclohexene in dichloromethane solutions at 25 °C, and under a hydrogen pressure of 5 bar. The yields of the catalytic hydrogenation reactions are summarized in Table 3. Complex **7**, as well as its homodinuclear analog $[\{\text{Pt}(\text{C}_6\text{H}_3(\text{CH}_2\text{NMe}_2\text{-}2,6)_2\})_2(\mu\text{-Hbiim})](\text{SO}_3\text{CF}_3)_2$ (**11**)

Table 3. Homogeneous hydrogenation of 1-hexene and cyclohexene catalyzed by complexes **1**, **7–9** and **11**

Catalyst	Hydrogenation of 1-hexene		Hydrogenation of cyclohexene	
	Time [h]	Yield of hexane (%)	Time [h]	Yield of cyclohexane (%)
$[\text{Os}(\text{H}_2\text{biim})_2(\text{O}=\text{PPh}_3)_2](\text{NO}_3)_3$ (1)	10	11	10	0
$[\{\text{Pt}\{\text{C}_6\text{H}_3(\text{CH}_2\text{NMe}_2\text{-}2,6)_2\})_2(\mu\text{-Hbiim})(\text{SO}_3\text{CF}_3)_2]$ (11)	5	2	5	3
$[\{\text{Pt}\{\text{C}_6\text{H}_3(\text{CH}_2\text{NMe}_2\text{-}2,6)_2\})_2(\mu\text{-Hbiim})_2\text{Os}(\text{O}=\text{PPh}_3)_2](\text{NO}_3)_3(\text{SO}_3\text{CF}_3)_2 \cdot 4\text{H}_2\text{O}$ (7)	5	7	5	3
$[\{\text{Pd}(\text{cod})\}_2(\mu\text{-biim})_2\text{Os}(\text{O}=\text{PPh}_3)_2](\text{NO}_3)_3$ (8)	10	53 ^[a]	10	36
$[\{\text{Pd}(\text{en})\}_2(\mu\text{-biim})_2\text{Os}(\text{O}=\text{PPh}_3)_2](\text{NO}_3)_3$ (9)	5	15	5	10

^[a] By-products: 29% 2-hexene, 18% 3-hexene. Note that the formation of by-products in all other experiments was negligible.

have a low catalytic activity. This is probably due to the inertness of these coordinatively saturated complexes towards ligand exchange. With $[\text{Os}(\text{H}_2\text{biim})_2(\text{O}=\text{PPh}_3)_2](\text{NO}_3)_3$ (**1**) as a catalyst, 11% of hexane was obtained from 1-hexene, but no hydrogenation was observed with cyclohexene. The most active catalyst in the series is $[\{\text{Pd}(\text{cod})\}_2\text{Os}(\mu\text{-biim})_2(\text{O}=\text{PPh}_3)_2](\text{NO}_3)_3$ (**8**) (Table 3). A probable mechanism for the catalytic cycle involves hydrogenation of 1,5-cyclooctadiene and the formation of a coordinatively unsaturated palladium center as the catalytically active species. This could explain the lower activity of $[\{\text{Pd}(\text{en})\}_2\text{Os}(\mu\text{-biim})_2(\text{O}=\text{PPh}_3)_2](\text{NO}_3)_3$ (**9**) since the chelating ligand en is not easily substituted by substrate molecules. An attempt to use the mononuclear complex $[\text{Pd}(\text{H}_2\text{biim})(\text{cod})](\text{NO}_3)_2$ (**12**) as a homogeneous catalyst under identical conditions was unsuccessful, as it decomposes under hydrogen with the formation of palladium metal. This adequately demonstrates the increased stability of the Pd(cod) fragment in the trinuclear compound **8** relative to the mononuclear precursor **12**.

Conclusions

Deprotonation of the 2,2'-biimidazole building block in $[\text{Os}(\text{H}_2\text{biim})_2(\text{O}=\text{PPh}_3)_2](\text{NO}_3)_3$ (**1**) provides a powerful route towards the preparation of the trimetallic $\text{Pt}^{\text{II}}-\text{Os}^{\text{III}}-\text{Pt}^{\text{II}}$ and $\text{Pd}^{\text{II}}-\text{Os}^{\text{III}}-\text{Pd}^{\text{II}}$ complexes **7–9**. The solid-state structural analysis of $[\{\text{Pt}\{\text{C}_6\text{H}_3(\text{CH}_2\text{NMe}_2-2,6)_2\}_2(\mu\text{-Hbiim})_2\text{Os}(\text{O}=\text{PPh}_3)_2](\text{NO}_3)(\text{SO}_3\text{CF}_3)_2\cdot 4\text{H}_2\text{O}$ (**7**) demonstrates that the two $[\text{Pt}\{\text{C}_6\text{H}_3(\text{CH}_2\text{NMe}_2-2,6)_2\}]^+$ moieties are *trans* to each other, as expected from the *trans*-deprotonated sites of the 2,2'-biimidazolato ligands in the starting material, as shown in the solid-state structure of $[\text{Os}(\text{Hbiim})_2(\text{O}=\text{PPh}_3)_2][\text{RhCl}_4\{\text{NH}(\text{CH}_3)_2\}_2]$ (**2b**). Cyclic voltammetric studies demonstrate that deprotonation of 2,2'-biimidazole and the coordination to a second metal ion result in a modification of the redox properties of the central osmium ion, and this is probably due to a change in the ligand field. The OsPd_2 complex $[\{\text{Pd}(\text{cod})\}_2(\mu\text{-biim})_2\text{Os}(\text{O}=\text{PPh}_3)_2](\text{NO}_3)_3\cdot\text{H}_2\text{O}$ (**8**) is shown to have considerable catalytic activity towards the homogeneous hydrogenation of linear and cyclic alkenes, e.g. 1-hexene and cyclohexene.

Experimental Section

Materials and Measurements: The complex $[\text{Os}(\text{H}_2\text{biim})_2(\text{O}=\text{PPh}_3)_2](\text{NO}_3)_3\cdot\text{H}_2\text{O}\cdot 0.5\text{CH}_3\text{OH}$ (**1**) was prepared by a published method.^[10] $[\text{Os}(\text{Hbiim})_2(\text{O}=\text{PPh}_3)_2](\text{NO}_3)_3\cdot 2\text{H}_2\text{O}$ (**2**) was obtained by reaction of **1** with KOH in methanol/dichloromethane.^[10] $[\text{Pt}\{\text{C}_6\text{H}_3(\text{CH}_2\text{NMe}_2-2,6)_2\}(\text{H}_2\text{O})(\text{SO}_3\text{CF}_3)$ (**4**) was prepared from $[\text{Pt}\{\text{C}_6\text{H}_3(\text{CH}_2\text{NMe}_2-2,6)_2\}\text{Cl}]^{\text{I}}^{\text{[15]}}$ (addition of AgSO_3CF_3 in methanol). $[\text{Me}_2\text{NH}_2][\text{RhCl}_4(\text{HNMe}_2)_2]^{\text{I}}^{\text{[16]}}$ was obtained as described elsewhere. ^1H , $^{13}\text{C}\{^1\text{H}\}$, and $^{31}\text{P}\{^1\text{H}\}$ NMR spectra were recorded with a Bruker AC 250 spectrometer, chemical shifts (^1H and ^{13}C) in ppm are quoted relative to SiMe_4 . ^{31}P chemical shifts are given in ppm with respect to 85% H_3PO_4 (^{31}P : $\delta = 0$) as an external

standard. Infrared spectra (KBr pellets) were recorded with a Perkin–Elmer 16PC FT-IR instrument. UV/Vis spectra were obtained with a Cary 1E spectrophotometer. Magnetic measurements were carried out with an Alfa MK 1 magnetic susceptibility balance. Electrochemical measurements (CV) were performed in methanol solutions containing $[\text{nBu}_4\text{N}]\text{PF}_6$ (0.1 mol·dm⁻³) at 293 K, using a BAS 100B system with a glassy carbon working electrode, a platinum auxiliary electrode and an Ag/AgCl reference electrode. All potentials are referenced to the ferrocene/ferrocenium couple ($E = 0.0$ V). GC-MS analyses were performed with a Fison GC 8000/MD 800 series instrument, equipped with a ZB-1 (Zebron) column. Melting (decomposition) points were determined with a Gallenkamp MFB 595 010 M melting point apparatus. Organic solvents (methanol, dichloromethane) were freshly distilled before use. Microanalyses were obtained from the microanalytical laboratory of the chemical institutes of the University of Heidelberg or the Technische Universität Bergakademie Freiberg.

X-ray Crystallography: X-ray quality crystals of $[\text{Os}(\text{Hbiim})_2(\text{O}=\text{PPh}_3)_2][\text{RhCl}_4\{\text{HN}(\text{CH}_3)_2\}_2]$ (**2b**) and $[\{\text{Pt}\{\text{C}_6\text{H}_3(\text{CH}_2\text{NMe}_2-2,6)_2\}_2(\mu\text{-Hbiim})_2\text{Os}(\text{O}=\text{PPh}_3)_2](\text{NO}_3)(\text{SO}_3\text{CF}_3)_2$ (**7**) were obtained by slow concentration of solutions of the complexes in a dichloromethane/methanol (4:1) mixture at 25 °C. Experimental crystal data are listed in Table 4 and geometric details are presented in Table 2. X-ray structural data were collected with a Bruker SMART CCD diffractometer. The unit cell parameters were checked for the presence of higher lattice symmetry.^[17] Data were corrected for absorption using SADABS.^[18] The structures were solved by direct methods (SHELX-97/2).^[19] Refinement was carried out by full-matrix least-squares techniques on F^2 (SHELXL-97/2).^[19] Hydrogen atoms were located from the difference Fourier map. All hydrogen atoms were fully refined. All non-hydrogen atoms were refined anisotropically.

Catalytic Hydrogenation of 1-Hexene and Cyclohexene: All experiments were performed in a 100-mL stainless steel autoclave with an inner polytetrafluorethylene vessel. In a typical experiment, 0.016 mmol of catalyst was placed as a solid in the autoclave, supplied with a magnetic stirring bar. Under stirring, the catalyst was dissolved in 6 mL of dichloromethane (complexes **7**, **8** and **11**) or in a mixture (90:10, 6 mL) of dichloromethane and methanol (complex **9**). 1-Hexene or cyclohexene (0.16 mmol; purity checked by GC-MS) was added to the solution of the catalyst. The autoclave was evacuated three times and filled with hydrogen. The pressure of hydrogen was increased to 5 bar. The reaction mixture was stirred for 5 h. The autoclave was then degassed and all volatile materials were evaporated from the reaction mixture using an oil-pump vacuum, and condensed (liquid nitrogen). The resulting solution was analyzed by GC-MS.

Synthesis of $[\text{Os}(\text{Hbiim})_2(\text{O}=\text{PPh}_3)_2][\text{RhCl}_4(\text{HNMe}_2)_2]$ (2b**):** $[\text{Os}(\text{Hbiim})_2(\text{O}=\text{PPh}_3)_2](\text{NO}_3)_3\cdot 2\text{H}_2\text{O}$ (**2**)^[10] (100 mg, 0.09 mmol) was treated with $[\text{Me}_2\text{NH}_2][\text{RhCl}_4(\text{HNMe}_2)_2]$ (33 mg, 0.09 mmol) in 20 mL of a dichloromethane/methanol (4:1) mixture at 25 °C. Slow evaporation of the solvent resulted in a mixture of solid products. This contained some of the starting materials, $\text{Me}_2\text{NH}_2\text{NO}_3$ and red crystals of **2b**, which were hand-picked and suitable for X-ray crystal structural analysis. Due to the very low yield, no further spectroscopic characterization was possible.

Synthesis of $[\{\text{Pt}\{\text{C}_6\text{H}_3(\text{CH}_2\text{NMe}_2-2,6)_2\}_2(\mu\text{-Hbiim})_2\text{Os}(\text{O}=\text{PPh}_3)_2](\text{NO}_3)(\text{SO}_3\text{CF}_3)_2\cdot 4\text{H}_2\text{O}$ (7**):** $[\text{Os}(\text{Hbiim})_2(\text{O}=\text{PPh}_3)_2](\text{NO}_3)_3\cdot 2\text{H}_2\text{O}$ (**2**, 200 mg, 0.18 mmol) was dissolved at 25 °C in 15 mL of a dichloromethane/methanol mixture (4:1). $[\text{Pt}\{\text{C}_6\text{H}_3(\text{CH}_2\text{NMe}_2-2,6)_2\}(\text{H}_2\text{O})(\text{SO}_3\text{CF}_3)$ (199 mg, 0.36 mmol), dissolved in methanol (5 mL), was added to the solution. The reac-

Table 4. Crystal data

	2b	7
Empirical formula	C ₅₂ H ₅₄ Cl ₄ N ₁₀ O ₂ OsP ₂ Rh	C ₇₄ H ₈₆ F ₆ N ₁₃ O ₁₅ OsP ₂ Pt ₂ S ₂
Formula mass [g/mol]	1347.90	2218.00
Crystal system	triclinic	triclinic
Space group	$P\bar{1}$	$P\bar{1}$
<i>a</i> [Å]	10.4293(5)	12.604(3)
<i>b</i> [Å]	10.6365(6)	13.471(3)
<i>c</i> [Å]	13.0287(7)	14.347(3)
α [°]	102.928(1)	63.919(4)
β [°]	91.684(1)	77.530(5)
γ [°]	109.854(1)	66.613(4)
<i>V</i> [Å ³]	1316.1(1)	2005.6(7)
<i>Z</i>	1	1
<i>T</i> [K]	103(2)	173(2)
Radiation used (λ [Å])	Mo-K α (0.70173)	Mo-K α (0.70173)
Reflection collected	22971	16683
Independent reflection	8886	11171
<i>R</i> (int)	0.0287	0.428
Linear absorption coefficient [mm ⁻¹]	3.040	5.237
<i>R</i> ^[a] [<i>I</i> > 2 σ (<i>I</i>)]/all	0.0238/0.0275	0.0487/0.1043
<i>wR2</i> ^[b] [<i>I</i> > 2 σ (<i>I</i>)]/all	0.0567/0.0592	0.1008/0.1191
Goodness-of-fit on <i>F</i> ²	1.055	0.958

[a] $R = \sum ||F_o| - |F_c|| / \sum |F_o|$. [b] $wR2 = [\sum w(F_o^2 - F_c^2)^2 / \sum w(F_o^4)]^{1/2}$.

tion mixture immediately changed from violet to red. The solution was stirred for 2 h, after which the volume was reduced to 4 mL. After 10 h at 25 °C, pale pink crystals of **7** precipitated. The slurry was decanted and the crystalline precipitate was washed twice with acetone (5 mL) and dried using an oil-pump vacuum to afford analytically pure **7**. Yield: 290 mg (0.13 mmol, 73% based on **2**). M.p. 219 °C (dec.). IR (KBr, cm⁻¹): $\tilde{\nu} = 1130 \nu_{(P=O)}$, 1276 $\nu_{(S=O)}$, 1385 $\nu_{a(NO_3^-)}$, 1439 $\nu_{(Ar,C=C)}$, 3075 $\nu_{(NH)}$. Due to paramagnetic line broadening no NMR spectra were recorded [molar magnetic susceptibility (powder, 298 K): $1.49 \times 10^{-3} \text{ cm}^3 \cdot \text{mol}^{-1}$]. UV/Vis (CH₂Cl₂): λ_{max} (ϵ , mol⁻¹·dm³·cm⁻¹) = 548 (6.2 × 10²), 375 nm (sh, 7.4 × 10³). CV (CH₃OH, 25 °C): $E_{1/2}(\text{Os}^{\text{III}}/\text{Os}^{\text{IV}}) = +0.53 \text{ V}$ ($\Delta E = 200 \text{ mV}$). C₇₄H₈₆F₆N₁₃O₁₅OsP₂Pt₂S₂ (2218.00): calcd. C 40.07, H 3.91, N 8.21; found C 40.04, H 3.85, N 8.47.

Synthesis of [Pd(cod)]₂(μ-biim)₂Os(O=PPh₃)₂(NO₃)₃·2H₂O (8**):** [Os(H₂biim)₂(O=PPh₃)₂](NO₃)₃ (**1**, (247 mg, 0.2 mmol) was dissolved in dichloromethane/methanol (4:1, 20 mL) at 25 °C. Potassium hydroxide (4.0 mL, 0.2 M in MeOH) was added. After stirring at room temperature for 15 min, [Pd(NO₃)₂(cod)] {0.40 mmol, prepared in situ by the reaction of [PdCl₂(cod)] (120 mg, 0.42 mmol) with AgNO₃ (143 mg, 0.84 mmol)} was added. The reaction mixture was stirred for 1 h. All volatile products were then removed using an oil-pump vacuum, and the remaining residue was extracted with dichloromethane (100 mL). The extract was filtered and dichloromethane was removed using an oil-pump vacuum to afford **8** as a dark green solid. Yield: 295 mg (0.178 mmol, 89% based on **1**). M.p.: gradual decomposition at > 150 °C. IR (KBr, cm⁻¹): $\tilde{\nu} = 1120 \nu_{(P=O)}$, 1184 $\nu_{a(NO_3^-)}$, 1436 $\nu_{(Ar,C=C)}$. ¹H NMR (CD₃OD): $\delta = 2.5$ (br. s, 16 H, CH₂, cod), 5.5 (br. s, 8 H, CH, cod), 7.5–7.8 (m, 34 H, C₆H₅, H₂-bim) ppm. ¹³C{¹H} NMR (CD₃OD): $\delta = 28.4$ (CH₂, cod), 76.4 (CH, cod), 129.9 (C-2,-2', biim²⁻), 130.1 (CH, C₆H₅), 133.1 (CH, C₆H₅), 133.8 (CH, C₆H₅), 136.4 (*i*-C, C₆H₅), 141.3 (C-5,-5', biim²⁻), 152.1 (C-4,4', biim²⁻) ppm. ³¹P{¹H} NMR (CD₃OD): $\delta = 32.6$ ppm. Molar magnetic susceptibility (powder, 298 K): $8.84 \times 10^{-4} \text{ cm}^3 \cdot \text{mol}^{-1}$. UV/Vis (CH₂Cl₂): λ_{max} (ϵ , L·cm⁻¹·mol⁻¹) = 351 (7.7 × 10³), 548 nm (3.9 × 10³). CV (CH₃OH): $E_{1/2}(\text{Os}^{\text{IV}}/\text{Os}^{\text{III}}) = +0.41 \text{ V}$ ($\Delta E = 280$

mV). C₆₄H₆₆N₁₁O₁₃OsP₂Pd₂ (1662.28): calcd. C 46.24, H 4.00, N 9.27; found C 45.81, H 4.16, N 9.25.

Synthesis of [Pd(en)]₂(μ-biim)₂Os(O=PPh₃)₂(NO₃)₃·H₂O (9**):** This complex was prepared from **1** (250 mg, 0.202 mmol) and [Pd(en)(H₂O)₂](NO₃)₂ (132 mg, 0.404 mmol), according to a procedure identical to that for **8**. A dark green solid was isolated. Yield: 270 mg (0.174 mmol, 87% based on **1**). M.p.: gradual decomposition at > 150 °C. IR (KBr, cm⁻¹): $\tilde{\nu} = 1118 \nu_{(P=O)}$, 1384 $\nu_{a(NO_3^-)}$, 1438 $\nu_{(Ar,C=C)}$. ¹H NMR (CD₃OD): $\delta = 2.96$ (br. s, 8 H, CH₂, en), 7.6–7.8 (m, 34 H, C₆H₅, H₂bim) ppm. ¹³C{¹H} NMR (CD₃OD): $\delta = 47.3$ (CH₂, en), 129.9 (C-2,-2', biim²⁻), 130.0 (CH, C₆H₅), 133.1 (CH, C₆H₅), 133.8 (CH, C₆H₅), 136.7 (*i*-C, C₆H₅), 141.1 (C-5,-5', biim²⁻), 152.6 (C-4,4', biim²⁻) ppm. ³¹P{¹H} NMR (CD₃OD): $\delta = 32.6$ ppm. Molar magnetic susceptibility (powder, 298 K): $1.07 \times 10^{-3} \text{ cm}^3 \cdot \text{mol}^{-1}$. UV/Vis (CH₂Cl₂): λ_{max} (ϵ , L·cm⁻¹·mol⁻¹) = 347 (7.1 × 10³), 547 nm (2.7 × 10³). CV (CH₃OH): $E_{1/2}(\text{Os}^{\text{IV}}/\text{Os}^{\text{III}}) = +0.23 \text{ V}$ ($\Delta E = 390 \text{ mV}$). C₅₂H₅₆N₁₅O₁₂OsP₂Pd₂ (1548.10): calcd. C 40.34, H 3.65, N 13.57; found C 40.48, H 3.72, N 13.15.

Synthesis of [Pt(C₆H₃(CH₂NMe₂-2,6)₂)]₂(μ-H₂biim)(SO₃CF₃)₂ (11**):** [Pt(C₆H₃(CH₂NMe₂-2,6)₂)Cl]^[15] (100 mg, 0.24 mmol) was dissolved in methanol (20 mL) and treated with AgOSO₂CF₃ (61 mg, 0.24 mmol). The reaction mixture was stirred for 12 h and AgCl was removed by filtration 2,2'-Biimidazole (16 mg, 0.12 mmol) was added to the filtrate and the reaction mixture was stirred for 10 h. After filtration, methanol was removed using an oil-pump vacuum to afford **11** as a gray solid. Yield: 120 mg {0.1 mmol, 84% based on [Pt(C₆H₃(CH₂NMe₂-2,6)₂)Cl]}. M.p. 214 °C (dec.). IR (KBr, cm⁻¹): $\tilde{\nu} = 1275 \nu_{(S=O)}$, 1441 $\nu_{(Ar,C=C)}$, 3080 $\nu_{(NH)}$. C₃₂H₄₄F₆N₈O₆Pt₂S₂ (1205.02): calcd. C 31.90, H 3.68, N 9.30; found C 31.52, H 4.05, N 8.95.

Acknowledgments

This work was supported in part by the Deutsche Forschungsgemeinschaft, the Fond der Chemischen Industrie and the

Alexander-von-Humboldt-Stiftung. We thank Mrs. Petra Krämer for help in performing the GC-MS analyses. We also would like to thank Degussa AG (Hanau) for the generous gift of OsO₄ and RhCl₃.

- [1] [1^a] R. Choukroun, D. Gervais, P. Kalck, F. Senocq, *J. Organomet. Chem.* **1987**, 335, C9–C12. [1^b] R. Mutin, C. Lucas, J. Thivole-Cazat, V. Dufand, F. Dany, J. M. Basset, *J. Chem. Soc., Chem. Commun.* **1988**, 896–898. [1^c] M. A. Esteruelas, M. P. Garcia, A. M. Lopez, L. Oro, *Organometallics* **1991**, 10, 127–133. [1^d] E. Sola, V. I. Bakhmutov, F. Torres, A. Elduque, J. A. Lopez, F. Lahoz, H. Werner, L. A. Oro, *Organometallics* **1998**, 17, 683–696.
- [2] [2^a] P. Kalck, *Polyhedron* **1988**, 7, 2441–2450. [2^b] A. Dedieu, P. Escaffre, J. M. Frances, P. Kalk, A. Thorez, *Nouv. J. Chem.* **1986**, 10, 631–696.
- [3] [3^a] S. W. Kaiser, R. B. Saillant, W. M. Butler, P. G. Rasmussen, *Inorg. Chem.* **1976**, 15, 2681–2687. [3^b] S. W. Kaiser, R. B. Saillant, P. G. Rasmussen, *J. Am. Chem. Soc.* **1975**, 97, 425–426. [3^c] S. W. Kaiser, R. B. Saillant, W. M. Butler, P. G. Rasmussen, *Inorg. Chem.* **1976**, 15, 2688–2694.
- [4] M. S. Haddad, D. N. Hendrickson, *Inorg. Chem.* **1978**, 17, 2622–2630.
- [5] R. Usón, J. Gimeno, J. Forniés, F. Martínez, *Inorg. Chim. Acta* **1981**, 50, 173–177.
- [6] A. Maiboroda, G. Rheinwald, H. Lang, *Inorg. Chem. Commun.* **2001**, 4, 381–383.
- [7] P. Majumdar, S.-M. Peng, S. Goswami, *J. Chem. Soc., Dalton Trans.* **1998**, 1569–1574.
- [8] M. P. Garcia, A. M. López, M. A. Esteruelas, F. J. Lahoz, L. A. Oro, *Chem. Commun.* **1988**, 793–795.
- [9] R. Usón, L. A. Oro, J. Gimeno, M. A. Ciriano, J. A. Cabeza, *J. Chem. Soc., Dalton Trans.* **1983**, 233–230.
- [10] A. Maiboroda, G. Rheinwald, H. Lang, *Eur. J. Inorg. Chem.* **2001**, 2263–2269.
- [11] L. Zsolnai, G. Huttner, *ZORTEP*, University of Heidelberg, **1994**.
- [12] C. M. Che, T. F. Lai, W. C. Chung, W. F. Schaefer, H. B. Grey, *Inorg. Chem.* **1987**, 26, 3907–3911.
- [13] M. A. Esteruelas, F. J. Lahoz, L. A. Oro, E. Onate, N. Ruiz, *Inorg. Chem.* **1994**, 33, 787–792.
- [14] G. Mesroni, E. Alessio, A. Sessanta o Santi, S. Geremia, A. Bergamo, G. Sava, A. Boccarelli, A. Schettino, M. Coluccia, *Inorg. Chim. Acta* **1998**, 273, 62–71.
- [15] J. Terheijden, G. Van Koten, F. Muller, D. M. Grove, K. Vrieze, E. Nielsen, C. H. Stam, *J. Organomet. Chem.* **1986**, 315, 401–417.
- [16] I. B. Bondarenko, N. A. Buzina, Yu. S. Varshavskii, M. I. Gel'fman, V. V. Razumovskii, T. G. Cherkasova, *Russ. J. Inorg. Chem.* **1971**, 16, 1629–1672.
- [17] A. L. Spek, *Acta Crystallogr., Sect. A* **1990**, 46, C34.
- [18] Area-Detector Absorption Corrections, Siemens Industrial Automation, Inc., Madison, WI, **1996**.
- [19] G. M. Sheldrick, *SHELX-97, Programs for Crystal Structure Analysis (Release 97–2)*, University of Göttingen, Germany, **1997**.

Received October 9, 2002